Novel Indazole Non-Nucleoside Reverse Transcriptase Inhibitors Using Molecular Hybridization Based on Crystallographic Overlays†

Lyn H. Jones,*,‡ Gill Allan,|| Oscar Barba,‡ Catherine Burt,# Romuald Corbau,§ Thomas Dupont,‡ Thorsten Knöchel,▽ Steve Irving,⊥ Donald S. Middleton,‡ Charles E. Mowbray,‡ Manos Perros,§ Heather Ringrose,○ Nigel A. Swain,‡ Robert Webster,|| Mike Westby,§ and Chris Phillips⊥

Discovery Chemistry, Discovery Biology, Pharmacokinetics, Dynamics, and Metabolism, Structural Biology, Molecular Informatics and Structure-Based Design, Sandwich Laboratories, Pfizer Global Research and Development, Ramsgate Road, Sandwich, Kent CT13 9NJ, United Kingdom

Received September 10, 2008

A major problem associated with non-nucleoside reverse transcriptase inhibitors (NNRTIs) for the treatment of HIV is their lack of resilience to mutations in the reverse transcriptase (RT) enzyme. Using structural overlays of the known inhibitors efavirenz and capravirine complexed in RT as a starting point, and structure-based drug design techniques, we have created a novel series of indazole NNRTIs that possess excellent metabolic stability and mutant resilience.

Introduction

Approximately 33 million people are living with HIV/AIDS worldwide, and 2.5 million people were newly infected with the virus in 2007.[1] HIV slowly attacks and destroys the immune system, leaving an individual open to other infections that eventually result in death. There is no cure for HIV infection, but a number of drugs slow or halt disease progression. However, HIV can rapidly become resistant to any single antiretroviral drug, therefore a combination of three or more drugs are usually required to effectively suppress the virus. This is known as highly active antiretroviral therapy (HAART).

Reverse transcriptase (RT[a]) is an essential enzyme in the infectious lifecycle of HIV, and inhibition of this enzyme has shown utility in the treatment of HIV. Several inhibitors of RT are used as components of HAART. However, established drugs called non-nucleoside reverse transcriptase inhibitors (NNRTIs), which bind to an allosteric pocket outside the catalytic site, are particularly vulnerable to the development of viral resistance caused by mutations in RT that can retain viable enzymatic function. The so-called first-generation NNRTIs such as nevirapine, delavirdine, and efavirenz (Figure 1) are very susceptible to single-point resistance mutations within RT and therefore significant efforts in this field have focused on developing second-generation NNRTIs with an improved mutant profile.[2] For example, treatment with efavirenz, the market leader in this class, can result in drug resistant virus due to the emergence of the K103N mutation in the NNRTI binding pocket of the enzyme.[3] Etravirine (Figure 1) is a recently launched second-generation NNRTI drug that retains activity against the clinically relevant mutations of RT, particularly K103N and Y181C.[4] However, there is still a need for additional novel chemical substrate that provides opportunities for delivering broad spectrum activity against mutant HIV. Our key aim has been the design and development of novel and potent NNRTIs that retain potent activity (within 10-fold of wild-type) against the most clinically relevant mutations, particularly K103N, thus reducing their intrinsic susceptibility to these mutations.

Capravirine (Figure 1) is a second-generation NNRTI which exhibits an improvement over the marketed NNRTIs with regard to its spectrum of activity against drug-resistant strains of HIV, including K103N.[5] We decided that capravirine was an appropriate starting point for our design of novel NNRTIs due to its excellent mutant profile and we reasoned that a hybrid of the well-established efavirenz template with that of capravirine (*molecular hybridization*[6]), facilitated by structure-based drug

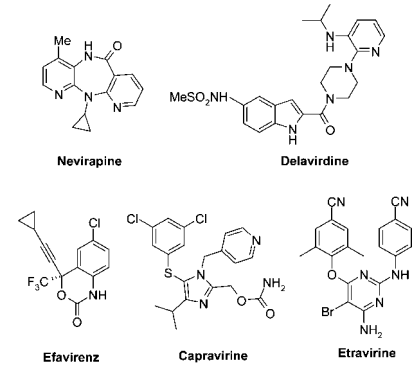

Figure 1. Existing NNRTIs.

† PDB code 2JLE for cocrystal **6** and K103N.

* To whom correspondence should be addressed. Phone: +44 (0)130-4644256. Fax: +44 (0)1304651821. E-mail: Lyn.Jones@pfizer.com.

‡ Discovery Chemistry.

§ Discovery Biology.

|| Pharmacokinetics, Dynamics and Metabolism.

⊥ Structural Biology.

Molecular Informatics and Structure-Based Design.

▽ Current address: Protein Crystallography (ZD-A/ZFA), Merck KgaA, Frankfurter Strasse 250, D-64293 Darmstadt, Germany.

○ Current address: Hamilton Robotics Ltd, Knights Court, Solihull Parkway, Birmingham Business Park B37 7WY, United Kingdom.

[a] Abbreviations: AcOH, acetic acid; APCI, atmospheric pressure chemical ionization; CCD, charge-coupled device; CPV, capravirine; DCM, dichloromethane; DMF, *N*,*N*-dimethylformamide; DMSO, dimethyl sulfoxide; EDTA, ethylenediaminetetraacetic acid; EFV, efavirenz; Et, ethyl; EtOAc, ethyl acetate; FCC, flash column chromatography; HAART, highly active antiretroviral therapy; Hheps, human hepatocytes; HLM, human liver microsomes; HMBC, heteronuclear multiple bond correlation; HSQC, heteronuclear single quantum coherence; IC_{50}, half-maximal (50%) inhibitory concentration; IR, infrared; LCMS, liquid chromatography mass spectrometry; MeCN, acetonitrile; mL, milliliter; μL, microliter; NBS, *N*-bromosuccinimide; NOE, nuclear Overhauser effect; Me, methyl; MeOH, methanol; MOI, multiplicity of infection; mp, melting point; nd, not determined; nM, nanomolar; NMR, nuclear magnetic resonance; NNRTI, non-nucleoside reverse transcriptase inhibitors; RPMI, Roswell Park Memorial Institute medium; RT, reverse transcriptase; THF, tetrahydrofuran; tBuOH, *tert*-butanol; TTP, thymidine-5′-triphosphate; wt, wild-type.

10.1021/jm801322h CCC: $40.75
Published on Web 01/28/2009

Scheme 1. Synthesis of 3-Methyl Indazoles[a]

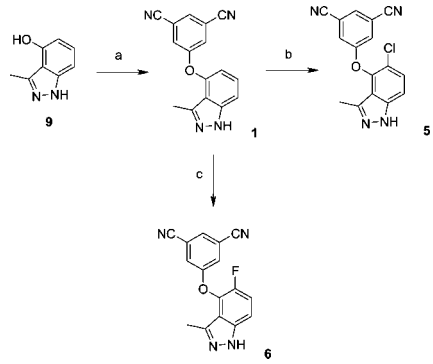

[a] Reagents and conditions: (a) 3,5-dicyanofluorobenzene, K_2CO_3, DMF, 80°C, 45%; (b) SO_2Cl_2, AcOH, 70°C, 35%; (c) Selectfluor, MeCN, rt, 56%.

Scheme 2. Synthesis of 3-Ethyl Indazoles[a]

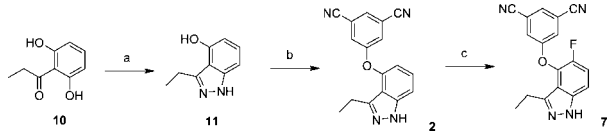

[a] Reagents and conditions: (a) $N_2H_4.H_2O$, ethylene glycol, 140°C, 92%; (b) 3,5-dicyanofluorobenzene, K_2CO_3, DMF, 75°C, 23%; (c) Selectfluor, MeCN, rt, 41%.

design, could create a novel starting point which may furnish analogues with the desired potency and resilience to RT mutations.

Synthetic Chemistry

At the outset, we desired a facile and reliable method for the preparation of 4-aryloxyindazoles, which would allow us to prepare a variety of related analogues in this series. Our strategy for their preparation involved the arylation of 4-hydroxy indazoles using an electron-deficient aryl fluoride as the key step. Treatment of the known 4-hydroxyindazole **9**[7] with commercially available 3,5-dicyanofluorobenzene provided the desired adduct **1** in modest yield (Scheme 1). Chlorination and fluorination of **1** provided derivatives **5** and **6**, respectively (structures confirmed by NOE and C−H correlation NMR experiments: see Supporting Information).

Similar chemistry was used to prepare the 3-ethyl indazole derivatives (Scheme 2). Treatment of the known resorcinol **10**[8] with hydrazine at high temperature effected transformation to indazole **11**. Arylation provided **2**, and fluorination of this derivative yielded **7**. Further modifications to the 3-position of the indazole were readily achieved by radical bromination of derivative **12**, which was reacted with methylamine and methanol to provide **3** and **4**, respectively (Scheme 3).

Modification of the 7-position of the indazole was realized using a selective bromination of **1**, (**14** structure confirmed by NOE: see Supporting Information), followed by a Stille reaction to install the ethylene group, followed by oxidative cleavage and reduction of the resulting aldehyde to provide derivative **8** (Scheme 4). Commercially available 3-indazolinone **15** was arylated with 3,5-dicyanofluorobenzene (in the same manner as **9**) to furnish **16** (Scheme 5).

Target Design

Our starting point was an analysis of the published X-ray cocrystal structures of efavirenz and capravirine with RT to investigate the relation between structure and function. The

Scheme 3. Modification of the Indazole 3-Position[a]

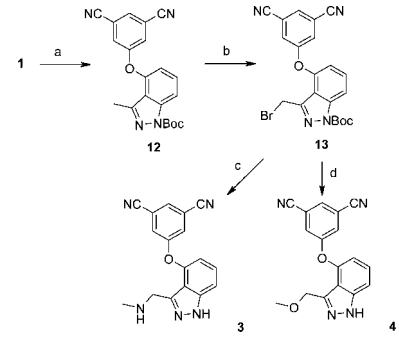

[a] Reagents and conditions: (a) Boc_2O, K_2CO_3, DMF, 40°C, 96%; (b) NBS, VAZO, CCl_4, reflux, 96%; (c) $MeNH_2$, THF, 66°C, 40%; (d) MeOH, NEt_3, 80°C, 50%.

Scheme 4. Modification of the 7-Position[a]

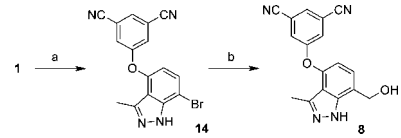

[a] Reagents and conditions: (a) Br_2, AcOH, rt, 92%. (b) (i) Tributylvinyltin, $Pd_2(dba)_3$, P(*o*-tolyl)$_3$, dioxane, reflux; (ii) OsO_4, NMO, ^{t}BuOH/THF/H_2O then $NaIO_4$; (iii) $NaBH_4$, MeOH, 45% over 3 steps.

Scheme 5. Synthesis of 3-Phenoxy Derivative **16**[a]

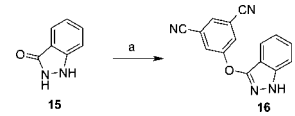

[a] Reagents and conditions: (a) 3,5-dicyanofluorobenzene, K_2CO_3, DMF, 75°C, 35%.

capravirine−RT complex (1EP4, Supporting Information), described previously by Stuart and Stammers, sheds light on the structural components responsible for its resilience to drug resistant mutations.[9] A key feature is the hydrogen bonding network capravirine makes with the peptide backbone of the NNRTI allosteric binding pocket. Two of these hydrogen bonds are between the carbamate group and the peptide main chain of residues K103 and P236. A third bond is formed between N3 of capravirine and the main chain of residue K101, which is mediated by a bridging water molecule. Interestingly, both the N−H and carbonyl groups of the cyclic carbamate substituent of efavirenz form direct hydrogen bonds with the K101 main chain atoms (1FKO, Supporting Information) without the need for a bridging water.[10]

Another key attribute of the capravirine−RT structure is an optimized edge-to-face π-interaction between the 3,5-dichlorophenyl substituent of capravirine and the indole moiety of the highly conserved residue W229. Indeed, the rational design of NNRTIs to interact specifically with W229 to improve mutant resilience has also been suggested by Balzarini and De Clercq[11] and was recently utilized in the development of pyrrolobenzoxazepine NNRTIs by Campiani and co-workers.[12] A crystallographic overlay of efavirenz and capravirine within the binding site is shown in Figure 2. This overlay nicely illustrates the key differences between these NNRTIs in the location and nature of the group, which occupies the lipophilic pocket created by W229, Y188, and Y181 in the allosteric binding site. Our initial aim was to transpose the 3,5-disubsituted phenyl moiety present in capravirine to a novel bicyclic template (similar to but distinct

Figure 2. Crystallographic overlay of efavirenz (gold) and capravirine (pink) with RT (protein removed for clarity).

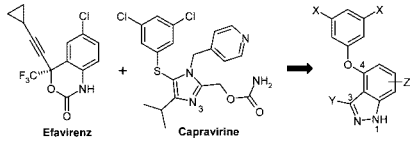

Figure 3. Molecular hybridization of capravirine and efavirenz to create the indazole template.

from the dihydrobenzoxazinone template of efavirenz), while ensuring the π-interaction with the immutable W229 residue could be retained. In particular, we were keen to avoid the chiral center present in efavirenz, thus reducing synthetic complexity, so the indazole template appeared to be ideally suited for our purposes because it could satisfy these structural criteria (Figure 3). Additionally, the N−H moiety of the indazole should undergo hydrogen bonding with the main chain of residue K101, similar to that in the efavirenz complex.

Results and Discussion

From the structural overlap shown in Figure 2, we noticed that the most favorable position for the incorporation of the 3,5-disubstituted benzene moiety into the indazole template would be the 4-position as this is closest to the location of this group in capravirine. For synthetic expedience, the first analogue we prepared in this series was **1** (Scheme 1). We have previously shown that a 3,5-dicyanophenoxy group can be incorporated into NNRTIs,[13] and amenable synthetic chemistry facilitated its incorporation into the indazole template. In fact, the replacement of the hydrophobic chlorine atoms with nitrile moieties (ΔLogP ~ -2 from Rekker fragments)[14] and removing the metabolically vulnerable sulfur atom with the more polar oxygen, creates a more "druggable" starting point for our design due to the expected improvements in metabolic stability and solubility associated with reducing lipophilicity (see below).[15]

Pleasingly, **1** possessed encouraging potency against wild-type RT (Table 1). To test the importance of the location of this moiety in the indazole template, we appended this group to the 3-position to provide **16**, but this derivative is approximately 100-fold less potent than **1** (wild-type RT IC_{50} 38 μM), thus illustrating the usefulness of the structural overlays.

However, we found that **1** formed a reactive metabolite conjugate that could be trapped with glutathione following incubation with human liver microsomes (HLMs), a feature that has been linked with hepato- and idiosyncratic toxicity.[16] Although the structure of this conjugate was not further characterized, there is an obvious similarity with 3-methyl indole, which exhibits toxicity due to H-atom abstraction from the methyl group, followed by single electron oxidation to form the electrophilic imine-methide.[17] We reasoned that alternative

Table 1. Potency of Indazole Derivatives against the Wild-Type Reverse Transcriptase Enzyme

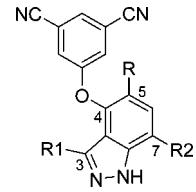

compd	R	R1	R2	wt IC_{50}/nM[a]
1	H	Me	H	332 (108)
2	H	Et	H	112 (2.2)
3	H	$MeNHCH_2$	H	>30000
4	H	$MeOCH_2$	H	1670 (3240)
5	Cl	Me	H	399 (195)
6	F	Me	H	50 (8.5)
7	F	Et	H	25 (9.6)
8	H	Me	CH_2OH	71 (2.0)

[a] Values are geomeans of three experiments. Standard deviations are in brackets.

groups at the 3-position of the indazole would avoid reactive metabolite formation by this mechanism. From the structural overlaps shown in Figure 2, we also noticed that a group here would overlap well with the CF_3-substituent in efavirenz and the isopropyl group in the 4-position of capravirine. Indeed, increasing the size of this substituent from a methyl to an ethyl group to provide **2** not only increased the potency 3-fold (Table 1), **2** was also negative in the reactive metabolite assay. Further elaboration of this substituent was pursued due to synthetic tractability, but we quickly discovered that increasing the size of this substituent even further resulted in significant potency reductions (**3** and **4**).

Additionally, from the crystallographic overlay in Figure 2, it was apparent that a hydrophobic group in the 5-position of the indazole would overlap well with the chloro-subsitituent in efavirenz. Interestingly, a chlorine atom at this position had minimal effect on potency (Table 1, compound **5**), but the smaller fluorine substituent improved the potency nearly 7-fold (compound **6**: see below for an explanation). Incorporating an ethyl group into the 3-position to provide **7** further improved the potency as we expected. Additionally, both **6** and **7** were negative in the reactive metabolite assay.

We were then able to cocrystallize **6**, as a representative from this series, with K103N RT as shown in Figure 4.[18] Derivative **6** makes the important edge-to-face π-interactions with the immutable W229 residue, and the indazole N−H undergoes a hydrogen bond with the peptide main chain of residue K101, thus satisfying both design features that were in our original plan.[19] The benzene ring also appears to make a face-to-face π-interaction with the Y188 residue, an interaction that has also been reported recently by Tucker and co-workers for a series of *meta*-cyanophenoxy-containing NNRTI derivatives.[20]

Table 2 shows the potency of derivatives **6** and **7** against the clinically relevant K103N and Y181C RT mutations (we have included efavirenz and capravirine for reference). Their balanced mutant profile (potencies within 10-fold of wild-type) and potent antiviral activity vindicates our original strategy. Interestingly, the highly mutable residue Y181 adopts a "down" position (Figure 4), analogous to a series of benzophenone NNRTIs recently reported by Stammers and co-workers, which appears to result from a steric clash between the *meta*-substituent on the A ring and the Y181 tyrosine. The resilience of these derivatives to the Y181C mutation may be due to a reduction in the aromatic stacking interactions with this residue, and that

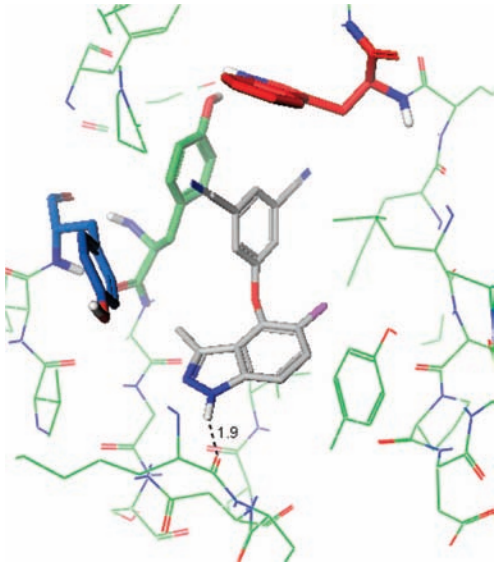

Figure 4. Cocrystal structure of **6** with K103N RT (2JLE). Highlighted residues: W229 (red); Y188 (green); Y181 (blue).

Table 2. Enzyme and Antiviral Potency and Metabolic Stability of Indazole Derivatives Capravirine and Efavirenz

compd	wt IC_{50}/nM[a]	K103N IC_{50}/nM[a]	Y181C IC_{50}/nM[a]	wt AV IC_{50}/nM[a]	HLM $T_{1/2}$/mins	HHeps $T_{1/2}$/mins
6	50 (8.5)	384 (30)	145 (83)	14 (8.4)	>120	>360
7	25 (9.6)	183 (80)	32 (16)	4.6 (1.1)	>120	>360
8	71 (2.0)	1268 (565)	nd[b]	14 (3.7)	>120	11
CPV	47 (35)	68 (60)	61 (66)	0.5 (0.5)	7.5	nd
EFV	14 (6.0)	364 (212)	40 (21)	0.4 (0.4)	nd	nd

[a] Values are geomeans of at least three experiments. Standard deviations are in brackets. **6**, **7**, and **8** were not cytotoxic, CC_{50} > 100 μM. [b] nd = not determined.

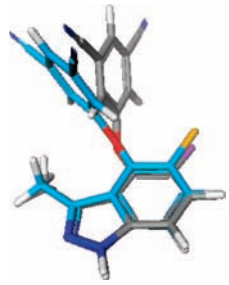

Figure 5. Overlay of **6** (gray; from cocrystal structure Figure 4, protein removed for clarity) and the energy minimized structure for **5** (blue).

efficient binding can still be achieved due to optimized interactions elsewhere (for example, the edge-to-face π-bond with W229).[21]

The conformation of compound **6** shown in Figure 4 was used as a template to generate an energy minimized structure for the chloro-derivative **5** (see Experimental Section), and the indazole rings of compounds **5** and **6** were then overlaid (Figure 5). As one might predict, the larger chlorine atom causes a flip and twist of the phenoxy group away from the halogen, implying that the conformation required for optimal binding is sterically less favored for **5** and may explain why this derivative is less potent than **6**.

We also noticed the potential for incorporating hydrogen-bonding groups into the benzene ring of the indazole template to mimic the carbamate substituent present in capravirine, which is apparent in the overlay shown in Figure 2. We felt these additional interactions may not only improve potency, but also augment resilience to mutations in RT. The 7-position of the indazole would appear to be the optimal location for a hydrogen-bonding group and derivative **8**, which contains a hydroxymethyl substituent at this position, displays a significant improvement in potency over **1** (~5-fold, Table 1). Interestingly, this derivative is >10-fold less potent against K103N (Table 2), unlike compounds **6** and **7**, and therefore optimization of the peptide-backbone hydrogen-bonding capacity would be required to address the apparent mutant vulnerability in this strategy. Compound **8** also retained excellent in vitro metabolic stability in human liver microsomes (Table 2). Metabolic stability was also assessed in vitro in human hepatocytes (HHeps), which retain phase 2 metabolic capabilities. Unfortunately, **8** was found to have poor stability in hepatocytes relative to **6** and **7** (Table 2) and therefore this derivative did not warrant further profiling.

Conclusion

We have used molecular hybridization of existing NNRTIs to efficiently create a new series of indazole derivatives that possess potent activity against both wild-type and clinically relevant mutations of the RT enzyme. Specifically, compounds **6** and **7**, fashioned using structure-based drug design, also possess potent antiviral activity and retain excellent in vitro metabolic stability. Because of the expense of HAART therapy, we have also addressed potential cost of goods issues in our design from the outset by pursuing a synthetically expedient series, which avoids chiral centers. These studies provide a proof-of-concept for the utility of molecular hybridization in the creation of novel leads as inhibitors of RT. Further development of this series will be reported in due course.

Experimental Section

The syntheses of compounds **1**, **5**, and **6** are described below as representatives of the series. Detailed syntheses of all other compounds, and procedures for the assays, crystallizations, and molecular modeling, are to be found in the Supporting Information.

5-(3-Methyl-1*H*-indazol-4-yloxy)-isophthalonitrile (1). 3-Methyl-4-hydroxyindazole (7.0 g, 47.3 mmol) was dissolved in DMF (100 mL), and potassium carbonate (6.5 g, 47.3 mmol) was added and stirred for 10 min before the addition of 3,5-dicyanofluorobenzene (6.9 g, 47.3 mmol). The mixture was then heated at 80 °C for 24 h, cooled to room temperature and concentrated in vacuo, then diluted with EtOAc, brine was added, and the layers separated, dried ($MgSO_4$), filtered, and concentrated under reduced pressure. The residue was purified by FCC (silica gel, 40% EtOAc/pentane) and crystallized from diethyl ether to yield the title compound as a white solid (5.8 g, 45%); mp 188−189 °C. ^{1}H NMR (400 MHz, $CDCl_3$) 7.62 (s, 1H), 7.48 (s, 2H), 7.40−7.35 (m, 2H), 6.67−6.63 (m, 1H), 2.48 (s, 3H). APCI MS *m*/*z* 275 $[M + H]^+$. LCMS CI *m*/*z* 275 $[M + H]^+$ >95%. Anal. ($C_{16}H_{10}N_4O$) C, H, N.

5-(5-Chloro-3-methyl-1*H*-indazol-4-yloxy)-isophthalonitrile (5). Indazole **1** (50 mg, 0.18 mmol) was dissolved in acetic acid (1 mL), SO_2Cl_2 (30 μL, 0.36 mmol) was added and stirred at 70 °C for 6 h, cooled to room temperature, concentrated in vacuo, diluted with DCM, washed with saturated aqueous sodium bicarbonate, dried ($MgSO_4$), filtered, and concentrated under reduced pressure. The residue was purified by FCC (silica gel, 25% EtOAc/pentane) to yield the title compound as a white solid (22 mg, 35%). ^{1}H NMR (400 MHz, CD_3OD) 7.87 (s, 1H), 7.52−7.44 (m, 4H), 2.39 (s, 3H). NOE and C−H correlation experiments included in Supporting Information. APCI MS *m*/*z* 309 $[M + H]^+$. LCMS CI *m*/*z* 309 $[M + H]^+$ >95%. Anal. ($C_{16}H_9N_4OCl$) C, H, N.

5-(5-Fluoro-3-methyl-1*H*-indazol-4-yloxy)-isophthalonitrile (6). Indazole **1** (100 mg, 0.34 mmol) was dissolved in MeCN (1 mL), Selectfluor (120 mg, 0.34 mmol) added, and the mixture stirred at room temperature for two days. Brine was then added and the mixture extracted with EtOAc, dried ($MgSO_4$), filtered, and

concentrated under reduced pressure. The residue was purified by FCC (silica gel, 20% EtOAc/toluene) to yield the title compound as a white solid (56 mg, 56%). ^{1}H NMR (500 MHz, DMSO-d_6) 13.01 (s, 1H), 8.19 (s, 1H), 7.88 (s, 2H), 7.45 (dd, *J* 9.3, 3.8 Hz, 1H), 7.41 (dd, *J* 9.6, 9.3 Hz, 1H), 2.30 (s, 3H). ^{13}C NMR (125 MHz, DMSO-d_6) 158.2, 147.6, 140.0, 139.5, 131.2, 130.5, 123.4, 116.5, 114.4, 109.2, 13.1. C−H correlation experiments included in Supporting Information. ^{19}F NMR (376 MHz, $CDCl_3$) −141.0. APCI MS *m*/*z* 293 $[M + H]^+$. LCMS CI *m*/*z* 293 $[M + H]^+$ >95%. Anal. ($C_{16}H_9FN_4O$) C, H, N.

Acknowledgment. We thank Michael Kinns and Torren Peakman for NOE and C−H correlation NMR experiments. We also thank Ian Burr, Alex Martin, and Amy Thomas for determining the potencies of these compounds and Iain Gardner for proof reading this manuscript.

Supporting Information Available: Detailed syntheses of all compounds (except **1**, **5**, and **6**), NOE and C−H correlation spectra of **5**, **6**, **14**, combustion analyses of **1**−**8** and **16**. Procedures for the enzyme and antiviral assays and molecular modeling details. X-ray diffraction data for **6** with K103N RT. Structures of efavirenz and capravirine with RT and overlays of compound **6** with efavirenz and capravirine. This material is available free of charge via the Internet at http://pubs.acs.org.

References

(1) UNAIDS/WHO *UNAIDS/WHO 2007 AIDS Epidemic Update*, **2007**.
(2) De Clercq, E. Non-Nucleoside Reverse Transcriptase Inhibitors (NNRTIs): Past, Present and Future. *Chem. Biodiversity* **2004**, *1*, 44–64.
(3) Bacheler, L.; Jeffrey, S.; Hanna, G.; D'Aquila, R.; Wallace, L.; Logue, K.; Cordova, B.; Hertogs, K.; Larder, B.; Buckery, R.; Baker, D.; Gallagher, K.; Scarnati, H.; Tritch, R.; Rizzo, C. Genotypic Correlates of Phenotypic Resistance to Efavirenz in Virus Isolates from Patients Failing Non-Nucleoside Reverse Transcriptase Inhibitor Therapy. *J. Virol.* **2001**, *75*, 4999–5008.
(4) Haubrich, R.; Gubernick, S.; Yasothan, U.; Kirkpatrick, P. Etravirine. *Nat. Rev. Drug Discovery* **2008**, *7*, 287.
(5) Fujiwara, T.; Sato, A.; El-Farrash, M.; Miki, S.; Abe, K.; Isaka, Y.; Kodama, M.; Wu, Y.; Chen, L. B.; Harada, H.; Sugimoto, H.; Hatanaka, M.; Hinumi, Y. S-1153 Inhibits Replication of Known Drug-Resistant Strains of Human Immunodeficiency Virus Type 1. *Antimicrob. Agents Chemother.* **1998**, *42*, 1340–1345.
(6) Viegas-Junior, C.; Danuello, A.; Bolzani, V.; Barreiro, E. J.; Fraga, C. A. M. Molecular Hybrization: A Useful Tool in the Design of New Drug Prototypes. *Curr. Med. Chem.* **2007**, *14*, 1829–1852.
(7) Boehm, H.-J.; Boehringer, M.; Bur, D.; Gmuender, H.; Huber, W.; Klaus, W.; Kostrewa, D.; Kuehne, H.; Luebbers, T.; Meunier-Keller, N.; Mueller, F. Novel Inhibitors of DNA Gyrase: 3D Structure Based Biased Needle Screening, Hit Validation by Biophysical Methods, and 3D Guided Optimization. A Promising Alternative to Random Screening. *J. Med. Chem.* **2000**, *43*, 2664–2674.
(8) Bobik, A.; Holder, G. M.; Ryan, A. Inhibitors of Hepatic Mixed Function Oxidase. 3. Inhibition of Hepatic Microsomal Aniline Hydroxylase and Aminopyrine Demethylase by 2,6- and 2,4-Dihydroxyphenyl Alkyl Ketones and Related Compounds. *J. Med. Chem.* **1977**, *20*, 1194–1199.
(9) Ren, J.; Nichols, C.; Bird, L. E.; Fujiwara, T.; Sugimoto, H.; Stuart, D. I.; Stammers, D. K. Binding of the Second Generation Non-Nucleoside Inhibitor S-1153 to HIV-1 Reverse Transcriptase Involves Extensive Main Chain Hydrogen Bonding. *J. Biol. Chem.* **2000**, *275*, 14316–14320.
(10) Ren, J.; Milton, J.; Weaver, K. L.; Short, S. A.; Stuart, D. I.; Stammers, D. K. Structural Basis for the Resilience of Efavirenz (DMP-266) to Drug Resistance Mutations in HIV-1 Reverse Transcriptase. *Structure* **2000**, *8*, 1089–1094.
(11) Pelemans, H.; Esnouf, R.; De Clercq, E.; Balzarini, J. Mutational Analysis of Trp-229 of Human Immunodeficiency Virus Type 1 Reverse Transcriptase (RT) Identifies This Amino Acid Residue as a Prime Target for the Rational Design of New Non-Nucleoside RT Inhibitors. *Mol. Pharm.* **2000**, *57*, 954–960.
(12) Fattorusso, C.; Gemma, S.; Butini, S.; Huleatt, P.; Catalanotti, B.; Persico, M.; De Angelis, M.; Fiorini, I.; Nacci, V.; Ramunno, A.; Rodriquez, M.; Greco, G.; Novellino, E.; Bergamini, A.; Marini, S.; Coletta, M.; Maga, G.; Spadari, S.; Campiani, G. Specific Targeting Highly Conserved Residues in the HIV-1 Reverse Transcriptase Primer Grip Region. Design, Synthesis and Biological Evaluation of Novel, Potent and Broad Spectrum NNRTIs with Antiviral Activity. *J. Med. Chem.* **2005**, *48*, 7153–7165.
(13) (a) Jones, L. H.; Allan, G.; Corbau, R.; Hay, D.; Middleton, D. S.; Mowbray, C. E.; Newman, S.; Perros, M.; Randall, A.; Vuong, H.; Webster, R.; Westby, M.; Williams, D. Optimization of 5-aryloxyimidazole non-nucleoside reverse transcriptase inhibitors. *ChemMedChem* **2008**, *3*, 1756–1762. (b) Jones, L. H.; Randall, A.; Barba, O.; Selby, M. Synthetic chemistry-led creation of a difluorinated biaryl ether non-nucleoside reverse transcriptase inhibitor. *Org. Biomol. Chem.* **2007**, *5*, 3431–3433. (c) Jones, L. H.; Dupont, T.; Mowbray, C. E.; Newman, S. A Concise and Selective Synthesis of Novel 5-Aryloxyimidazole NNRTIs. *Org. Lett.* **2006**, *8*, 1725–1727. (d) Jones, L. H.; Mowbray, C. E. A concise synthesis of trifluormethyl-substituted 4-aryloxy pyrazoles. *Synlett* **2006**, *9*, 1404–1406.
(14) Rekker, R. *The Hydrophobic Fragmental Constant*; Elsevier: Amsterdam, 1977.
(15) Bu, H.-Z.; Pool, W. F.; Wu, E. Y.; Raber, S. R.; Amantea, M. A.; Shetty, B. V. Metabolism and excretion of capravirine, a new non-nucleoside reverse transcriptase inhibitor, alone and in combination with ritonavir in healthy volunteers. *Drug Metab. Dispos.* **2004**, *32*, 689.
(16) Evans, D. C.; Watt, A. P.; Nicoll-Griffith, D. A.; Baille, T. A. Drug−Protein Adducts: An Industry Perspective on Minimizing the Potential for Drug Bioactivation in Drug Discovery and Development. *Chem. Res. Toxicol.* **2004**, *17*, 3–16.
(17) Kalgutkar, A. S.; Gardner, I.; Obach, R. S.; Shaffer, C. L.; Callegari, E.; Henne, K. R.; Mutlib, A. E.; Dalvie, D. K.; Lee, J. S.; Nakai, Y.; O'Donnell, J. P.; Boer, J.; Harriman, S. P. A comprehensive listing of bioactivation pathways of organic functional groups. *Curr. Drug Metab.* **2005**, *6*, 161–225.
(18) Coordinates have been deposited with the PDB and have the assigned code 2JLE.
(19) The crystallographic overlay of **6** with capravirine and efavirenz fits perfectly the predicted binding mode: see Supporting Information.
(20) Tucker, T. J.; Saggar, S.; Sisko, J. T.; Tynebor, R. M.; Williams, T. M.; Felock, P. J.; Flynn, J. A.; Lai, M.-T.; Liang, Y.; McGaughey, G.; Liu, M.; Miller, M.; Moyer, G.; Munshi, V.; Perlow-Poehnelt, R.; Prasad, S.; Sanchez, R.; Torrent, M.; Vacca, J. P.; Wan, B.-L.; Yan, Y. The design and synthesis of diaryl ether second generation HIV-1 non-nucleoside reverse transcriptase inhibitors (NNRTIs) with enhanced potency versus key clinical mutations *Bioorg. Med. Chem. Lett.* **2008**, *18*, 2959−2966. These authors observed a notable reduction in potency for their lead compound against the clinically rare mutation Y181L, presumably due to interactions between the compound and the Y188 residue. We cannot rule out a similar mutant vulnerability as we have not measured Y188 mutant potencies.
(21) Ren, J.; Chamberlain, P. P.; Stamp, A.; Short, S. A.; Weaver, K. L.; Romines, K. R.; Hazen, R.; Freeman, A.; Ferris, R. G.; Andrews, C. W.; Boone, L.; Chan, J. H.; Stammers, D. K. Structural basis for the improved drug resistance profile of new generation benzophenone non-nucleoside HIV-1 reverse transcriptase inhibitors. *J. Med. Chem.* **2008**, *51*, 5000–5008.

JM801322H